euspen's 25th International Conference & Exhibition, Zaragoza, ES, June 2025
www.euspen.eu

Influence of radial spindle error motions on the slot width when micro milling

Felix Zell[1], Sonja Kieren-Ehses[1], Benjamin Kirsch[1], Jan C. Aurich[1]

[1]*RPTU Kaiserslautern, Institute for Manufacturing Technology and Production Systems*

felix.zell@rptu.de

Abstract

Micro milling is a typical process for manufacturing micro slots for biomedical and microelectronics applications. The milling strategy and the spindle properties are essential to ensure high dimensional accuracy and surface quality. The most relevant spindle properties are the spindle error motions, i.e., deviations in the rotation of the spindle from the intended path. During milling the process forces can increase the spindle error motions. As a result, these error motions lead to deviations in the geometry of the milled slots. However, it still needs to be fully understood how the radial spindle error motions and, in general, how the overall run-out affect the milled slot width. Several factors contribute to the current incomplete understanding of the described correlations. For example, the spindle properties are most commonly analyzed in a non-contact state, where the micro end mill or artifact is not in contact with the workpiece. Therefore, comparing the spindle error motions measured in a non-contact state with the milled slot width is inaccurate. This research aimed to analyze the influence of radial spindle error motions on the slot width when micro milling. To do this, the radial error motions and the process forces were measured during milling experiments in brass. Afterward, the milled slot widths were evaluated. By comparing the three datasets, the understanding of the correlations between spindle error motions, process forces, and slot width deviations is extended.

Measurement; Micromachining; Milling; Spindle

1. Introduction

Micro milling is a precision manufacturing process widely used in industries such as biomedical and microelectronics [1]. Achieving dimensional accuracy and superior surface quality in this process depends on understanding the effects of several dynamic and geometric factors. Among these, spindle error motion and tool deflection are critical in influencing machining results such as surface finish, slot width and overall process stability [2].

Run-out, which refers to the eccentric motion of the cutting tool relative to its intended axis of rotation, directly impacts the surface finish and accuracy of the machined features. Schmitz et al. highlight the importance of run-out in milling, discussing its effects on surface position error, finish, and process stability [3].

In micro milling, tool run-out, combined with the minimum chip thickness effect, leads to material removal variations, affecting slot width and surface generation. Chen et al. developed models to describe these interactions, providing insight into how run-out affects machining accuracy [4]. Similarly, Zhang et al. investigated cutting forces and tool deflection, highlighting the need to consider run-out when predicting tool behavior during micro milling [5].

Dow et al. predicted the tool deflection for two micro milling scenarios based on cutting force models and calculated tool stiffness. With this indirect approach to tool deflection, they significantly improved the accuracy in their experiments with an open-loop compensation technique for the tool path. [6]

The process stability and the influence of run-out and dynamic tool deflection were investigated by Wang et al. They used displacement measurements of the tool deflection at tool point for their comprehensive micro-milling force model. [7]

Balázs et al. explored the interactions between cutting forces, vibration, and material properties in experiments. Because they used relatively large micro end mills (D = 500 µm), their findings may not be directly transferable to micro end mills < 100 µm. [8]

There is a lack of experimental studies, especially for very small micro end mills (D < 100 µm), which are particularly affected by deflections of the tool tip due to their low stiffness. This study aims to analyze the impact of spindle error motion and run-out on slot width in micro milling processes, providing critical insights for optimizing precision machining.

2. Experimental setup

The micro milling experiments were carried out on the nano grinding center (NGC), a desktop sized machine tool developed at our institute. The air-bearing spindle (spindle speed range 10 000 min^{-1} to 160 000 min^{-1}) has a maximum run-out of 2 µm at the applied spindle speed of 30 000 min^{-1}. The setup can be found in Figure 1.

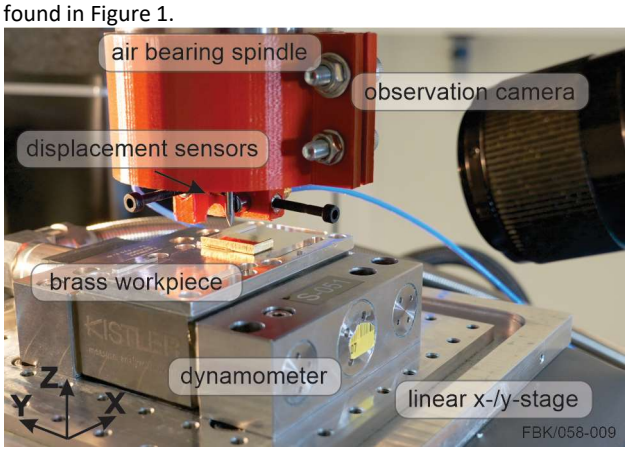

Figure 1. Setup used for the micro milling experiments.

2.1. Workpiece

The workpiece material used for the micro milling experiments was brass (CuZn39Pb2) with a size of 10 mm x 20 mm x 3 mm.

To ensure a flat surface of the specimen and the orthogonal alignment between tool and specimen, it was face milled on the NGC prior to the micro milling tests. This was done with a micro end mill with two cutting edges and a diameter of 3 mm.

2.2. Micro end mill

The tool used for the micro milling experiments was a single edged uncoated micro end mill made of cemented carbide (91 % WC, 9 % Co, grain size 0.2 µm). The micro end mill was manufactured to have a nominal effective cutting diameter of 50 µm, a helix angle of 0°, and a minor cutting edge angle of 12°. For detailed information on the manufacturing of the micro end mill, we refer to [9]. See Figure 2 for a SEM image of the micro end mill before deployment.

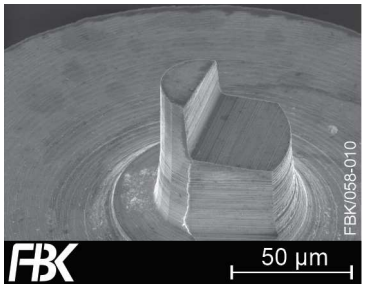

Figure 2. SEM-image of micro end mill.

2.3. Process parameters

In this study, slots have been milled across the whole width of the brass workpiece. Each slot was 10 mm long, and the feed was oriented along the x-axis. The spindle speed was kept constant at 30 000 min^{-1}, while the feed per tooth f_z was increased from 1 µm to 5 µm in increments of 1 µm. The cutting depth was kept at 5 µm for the first test series and increased to 10 µm for a second test series. However, this second test series was aborted due to tool breakage while milling the first slot at f_z = 1 µm. The single data point for the higher cutting depth (a_p = 10 µm, f_z = 1 µm) was still included in the results.

The spindle was warmed up for a few minutes until a stable thermal state had been reached. The test series was carried out with one tool and without reclamping the tool or the workpiece so that the clamping error did not influence the measurement results. The influence of wear was neglected, as the total machined feed travel was small, and abrasive wear could, therefore, be excluded.

3. Methods

During micro milling of the slots the occuring process forces were measured utilizing a piezoelectric multicomponent dynamometer (KISTLER[1] Type 9119AA1) and the run-out at the tool shank via a capacitive displacement measurement system (Micro-Epsilon[1] capaNCDT 6222/DL 6222). To analyze the widths of the milled slots, confocal microscope images were taken using a Nanofocus[1] OEM microscope. A 60x objective lens with a numerical aperture of 0.9 was used. The measuring field was1 020 µm x 268 µm. Detailed information about the analysis procedures is given in the following sections.

3.1. Measurement setup

To measure the process forces in x-, y- and z-direction the specimen was mounted on top of the dynamometer, which was mounted on top of the linear x-/y-stage (see Figure 1).

Due to the small cutting diameter it was not possible to measure the run-out at the tool tip directly. Instead the two displacement sensors were fixed to the spindle body and aligned to measure the run-out along the x- and y-axis at the tool shank with a diameter of 3 mm. It was assumed that no error movements between the spindle body and the workpiece exist. Due to geometrical restrictions the two sensors were offset along the z-axis by 5.5 mm. The sensor measuring along the x-axis was positioned 6 mm above the tool tip.

3.2. Signal processing

All analog sensor signals, three forces and two displacements, were simultaneously digitized with the same DAQ (National Instruments[1] NI 9205) at a sampling rate of 50 000 samples/s. The digitized voltage signals from the measurement systems were high-pass and low-pass filtered (Butterworth filter, cut-off frequency 1 Hz and 6 000 Hz). The filtered signals were then converted to force/displacement data using a conversion factor/calibration graph. Finally, the root mean square values were calculated with a moving window width of one revolution (100 data points).

Since the measurement data also contained values where the tool was not engaged (measurement lead and trail), the data was further processed using a MATLAB[1] script. Based on a defined threshold and the force signal in the y-direction F_y, the measurement data range in which the tool was engaged was determined. The first and last 10% were truncated to exclude transient processes at the beginning and end of tool engagement. The range determined with F_y was applied to the remaining data and the corresponding mean values and standard deviations were calculated. The data analysis method is illustraded in Figure 3 for F_y for the experiment with a_p = 5 µm and f_z = 1 µm.

For the run-out data, only the additional run-out, i.e., the tool deflection during micro milling, was of interest. Therefore, the baseline run-out was determined as the mean value over 90 % of the measurement lead and was subtracted from the run-out during milling.

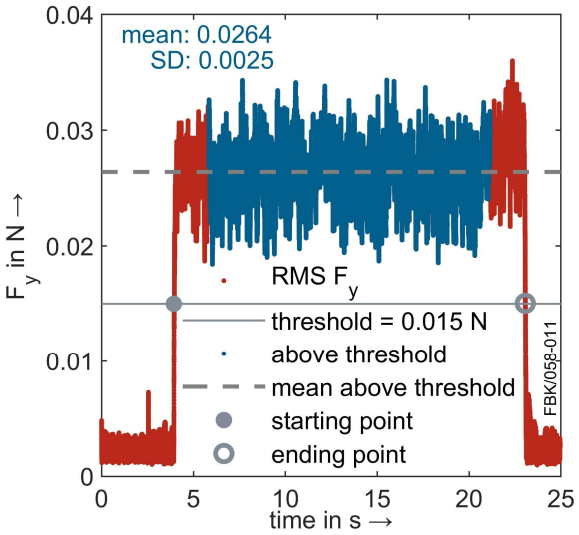

Figure 3. Data analysis for F_y in the case of a_p = 5 µm and f_z = 1 µm.

3.3. Analyzing slot widths

To evaluate the slot width, confocal microscope images of the milled slots were taken (see Figure 4 a) and processed using MountainsMap[1]. For each slot, profile sections from three re-

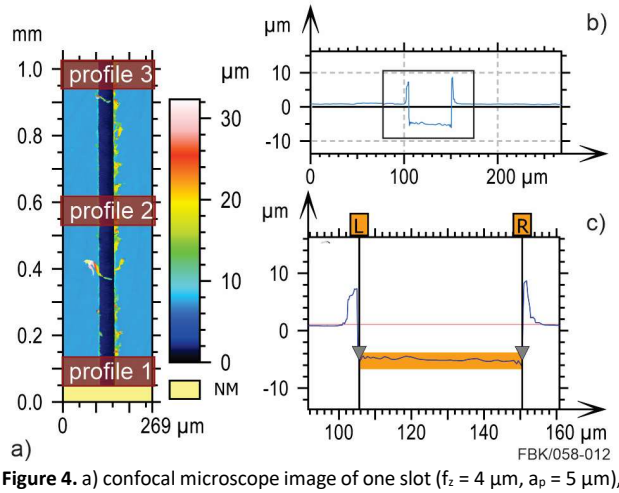

Figure 4. a) confocal microscope image of one slot (f_z = 4 µm, a_p = 5 µm), b) height profile extracted at upper position, c) definition of slot edges.

gions (start, middle, end) were extracted. The exact positioning of the profile section along the slot was done manually within the marked regions. This was done to ensure selection of complete profiles. Such a profile is shown in Figure 4 b). The slot width of each profile was determined based on the position of the left and right slot edge in the height profiles (see Figure 4 c). Then the mean and standard deviation was calculated for each slot.

4. Results

Figure 5 shows the mean values of the measured forces with the corresponding standard deviations during micro milling of the different slots. The measured forces range from approximatly 0.020 N to 0.060 N for F_x and F_y and 0.005 N to 0.012 N for F_z. All datasets show a clear trend of rising forces as f_z is increased. The coefficients of determination for the linear fits of the three datasets with $a_p = 5\mu m$ are very high (R^2 between 0.996 and 0.982 for F_y and F_z respectively). While for F_x and F_y increasing the cutting depth a_p to 10 µm leads to a significant rise of the forces, F_z slighty decreases compared to $a_p = 5$ µm and $f_z = 5$ µm. The mean forces and standard deviations for x- and y-direction are similar, whereas the mean values of F_z are only about 20-25 % as high.

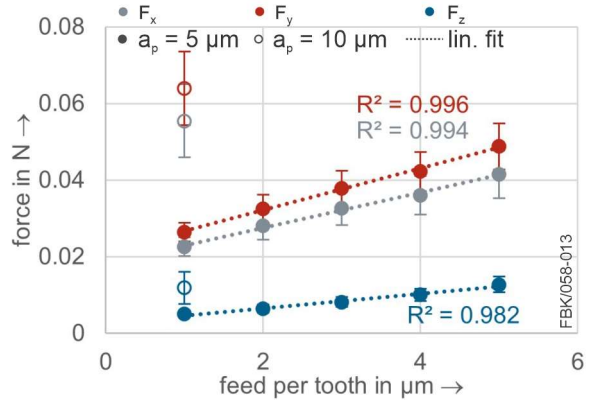

Figure 5. Process forces during micro milling.

Figure 6 shows the tool deflection at the tool shank during micro milling. The tool deflection increases almost linearly as f_z is increased. This is confirmed by the very high R^2 values (0.992 and 0.997) of the linear fits in x- and y-direction. The values for the x-direction are almost twice as high compared to the values for the y-direction, ranging from 0.035 µm to 0.090 µm and 0.015 µm to 0.050 µm respectively, and the measurements are characterized by a high amount of uncertainty.

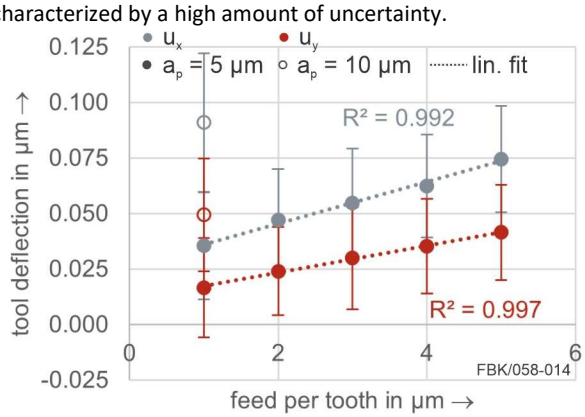

Figure 6. Tool deflection during micro milling.

For the experiment with $a_p = 10$ µm the tool deflection also lies higher than for $a_p = 5$ µm and $f_z = 5$ µm, but the difference is not quite as pronounced.

The slot depths for the five slots milled with a nominal cutting depth $a_p = 5$ µm are very similar and are on average 5.6 µm to 6.0 µm deep. The slot widths are shown in Figure 7. The measured slot widths range from approximatly 43.4 µm to 44.8 µm. In general, the slot widths also increase with increasing f_z. However, the correlation is not as clear as for the forces or tool deflections previously presented. This is also indicated by the significantly lower $R^2 = 0.830$ compared to $R^2 > 0{,}98$ for the process forces and tool deflections.

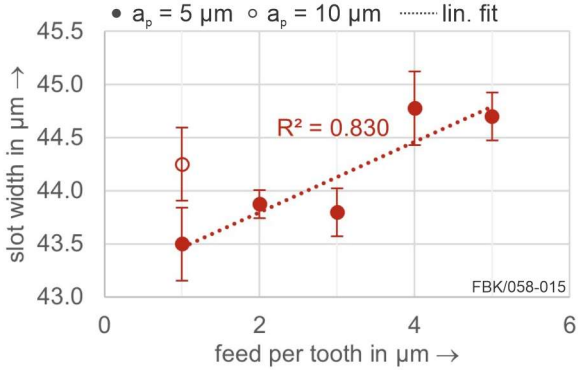

Figure 7. Evaluated widths of the milled slots.

To investigate, if there is also a strong correlation between the tool deflections and the process forces, u_x (u_y) have been plotted over F_x (F_y) and linear fit functions were calculated (this time including the data point $f_z = 1$ µm, $a_p = 10$ µm) – see Figure 8. The resulting coefficients of determination are very high (0.981 and 0.963 for $u_x(F_x)$ and $u_y(F_y)$ respectively) and indicate a strong correlation.

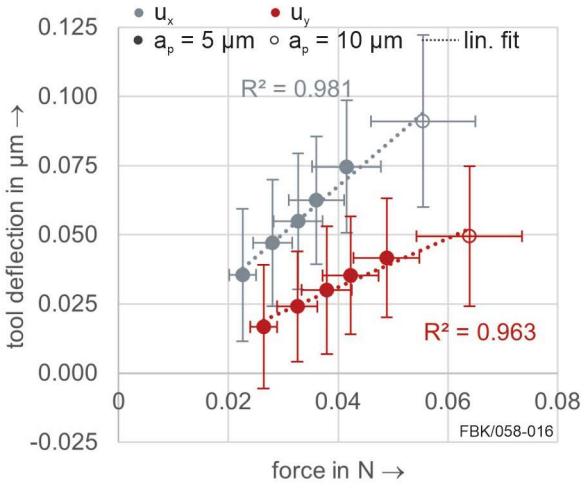

Figure 8. Tool deflection during micro milling as a function of the process forces.

Finally, the slot widths are evaluated as functions of the tool deflection and the process force in the y-direction, which corresponds to the orientation of the slot width (see Figure 9).

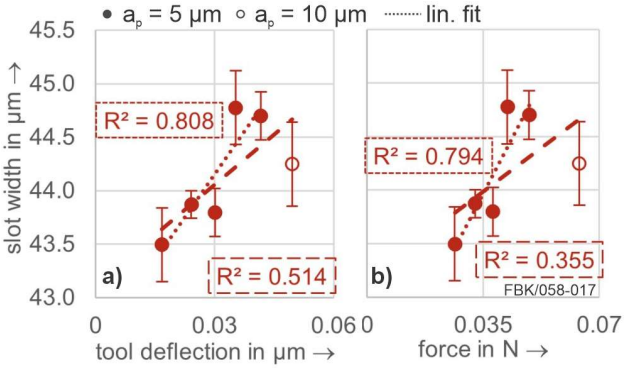

Figure 9. Slot widths as a function of a) the tool deflection and b) the process forces.

Similar to the findings earlier (Figure 7) the correlation of the slot width and the tool deflection as well as the process forces is not as clear. R^2-was calculated to just 0.808 and 0.794 for tool deflection and force respectively.

5. Discussion

Regarding the process forces, the observations made in this study are largely consistent with the expectations for micro milling. F_z, which corresponds to the passive forces, are in the expected ratio of 1:4 compared to F_x and F_y. F_y (forces oriented perpendicular to the feed direction are higher than F_x (forces oriented along the feed direction). This might be partially caused by reaction forces occurring due to ploughing effects before the minimum chip thickness for each cut (i.e., revolution) is reached.

Even though the tool deflections u_x and u_y measured at the tool shank are small (< 0.1 µm and thus in the range of the resolution limit of the measuring system) and characterized by high measuring uncertainties, a strong correlation with the feed per tooth could be demonstrated. The fact that u_y is smaller than u_x, despite F_y being larger than F_x, might be caused by two reasons. First, the sensor in the y-direction was positioned 5.5 mm further from the tool tip than the sensor in the x-direction, so that potential tilt of the spindle rotor would reduce u_y compared to u_x. Second, the spindle could exhibit structural asymmetry. However, this effect can most likely be neglected for this specific spindle. Structural asysmmetry can be evaluated by comparing the run-out in the x- and y-direction in the same measuring plane. This was achieved by measuring the run-out of the spindle in free-running condition, rotating the sensor fixture by 90° and measuring again. At a speed of 30,000 min^{-1} the deviations due to asymmetry were calculated to be lower than 2 % of the total run-out.

We found a strong correlation between the tool deflections and the process forces. The additional data point outside the test series with a_p = 5 µm was also mapped very well by the linear fit function. This indicates that the tool deflections were caused by the process forces directly. Whether the process forces were increased by a higher a_p or f_z does not seem to have an influence on the extent of the tool deflections.

While the difference between the smallest and largest average slot width found is about 1.3 µm, the measuring uncertainties are in the same order of magnitude. This might be due to two reasons. One, the method for analyzing the slot width by manually selecting three specific positions out of the confocal microscope images of the slots is prone to subjective errors and only reflects the slot width at individual points. Burrs can also restrict the selection of points, because they shade the underlying slot and slot edge. Two, other factors, e.g. the micro-structure in the current cutting area or temporary built-up edges could have a strong impact on the resulting slot width. Another aspect that points to the influence of other, unaccounted for influences is that the variance of the slot width is about 10 to 30 times larger than the measured tool deflections.

6. Conclusion and Outlook

In this study, we analyzed the interactions between the process forces, the tool deflections and the slot widths based on micro milling experiments.

To this end, the test setup including tool and workpiece, process parameters, measurement technology used, and evaluation methodology were described. The sensor signals were digitized and processed to extract the relevant information from the overall data. The methodology for evaluating the slot width based on confocal microscopy images was introduced.

It was shown that the process forces occurring in the x and y directions were between approximately 0.020 N and 0.060 N and showed a strong correlation with f_z (confirmed by $R^2 > 0.98$). A strong correlation with f_z was also found for the tool deflections ($R^2 > 0.99$), which were between 0.035 µm and 0.01 µm.

Despite comparatively large measurement uncertainties and various underlying influences (e.g. low stiffness of the micro end mill), a strong linear correlation was also found for the relationship between tool deflections and process forces ($R^2 > 0.96$). Higher process forces, regardless of their origin, seem to cause linearly higher tool deflections. However, the interactions between the tool deflections or process forces and the slot widths are not as clear (max. $R^2 \approx 0.8$). The individual process parameters appear to have a direct influence on the slot width that is not fully captured by the process result variables (forces, tool deflections).

Expanding the process parameter space investigated (to include other spindle speeds, depths of cut, and feeds per tooth) is the next step to improve the understanding of the interactions of the various process variables in micro milling. Also, improving the methodology for evaluating the slot width towards a more robust, area-based evaluation of the slot width over the entire length of the slot instead of individual positions to ensure reliable and repeatable determination of slot widths.

Acknowledgment

This research was funded by the Deutsche Forschungsgemeinschaft (DFG, German Research Foundation) – 491400446.

[1]Naming of specific manufacturers is done solely for the sake of completeness and does not necessarily imply an endorsement of the named companies nor that the products are necessarily the best for the purpose.

References

[1] Uhlmann E, Mullany B, Biermann D, Rajurkar K P, Hausotte T and Brinksmeier E 2016 Process chains for high-precision components with micro-scale features CIRP Annals **65** 549–572

[2] O'Toole L, Kang C-W and Fang F-Z 2021 Precision micro-milling process: state of the art Advances in manufacturing **9** 173–205

[3] Schmitz T L, Couey J, Marsh E, Mauntler N and Hughes D 2007 Runout effects in milling: Surface finish, surface location error, and stability International Journal of Machine Tools and Manufacture **47** 841–851

[4] Chen W, Huo D, Teng X and Sun Y 2017 Surface Generation Modelling for Micro end Milling Considering the Minimum Chip Thickness and Tool Runout Procedia CIRP **58** 364–369

[5] Zhang X, Yu T and Wang W 2018 Prediction of cutting forces and instantaneous tool deflection in micro end milling by considering tool run-out International Journal of Mechanical Sciences **136** 124–133

[6] Dow T A, Miller E L and Garrard K 2004 Tool force and deflection compensation for small milling tools Precision Engineering **28** 31–45

[7] Wang D, Penter L, Hänel A, Yang Y and Ihlenfeldt S 2022 Investigation on dynamic tool deflection and runout-dependent analysis of the micro-milling process Mechanical Systems and Signal Processing **178** 109282

[8] Balázs B Z, Geier N, Pereszlai C, Poór D I and Takács M 2021 Analysis of cutting force and vibration at micro-milling of a hardened steel Procedia CIRP **99** 177–182

[9] Aurich J C, Reichenbach I G and Schüler G M 2012 Manufacture and application of ultra-small micro end mills CIRP Annals **61** 83–86